Published in final edited form as:

*Phys Med Biol*. 2012 February 07; 57(3): 771–783. doi:10.1088/0031-9155/57/3/771.

# The Potential for Cerenkov luminescence imaging of alpha emitting isotopes

**NL Ackerman**[1] and **EE Graves**[2]

[1]Department of Physics, Stanford University, Stanford, CA 94305-4060

[2]Department of Radiation Oncology and Molecular Imaging Program, Stanford University School of Medicine, Stanford, CA 94305-5847

## Abstract

Cerenkov luminescence imaging (CLI) has been shown to have potential to image $\beta^+$and $\beta^-$emitting radioisotopes. This paper addresses the ability to use CLI to image 5 $\alpha$-emitters that have therapeutic potential. While none of the $\alpha$-particles have a sufficient velocity to directly produce Cerenkov light, all isotopes considered either have a second decay mode that produces Cerenkov or progeny that do. Monte Carlo studies show that $^{225}$Ac, $^{213}$Bi, and $^{212}$Bi can be easily imaged with CLI while $^{230}$U and $^{211}$At produce little light. Time effects are observed that must be taken into account when imaging these isotopes, which are not present with $\beta^{\pm}$-emitters like $^{18}$F.

### Keywords

Cerenkov; $^{225}$Ac; Radioimmunoimaging; Radionuclide Therapy; Radiopharmaceuticals

## 1. Introduction

Nuclear medicine uses radioisotopes for both imaging and therapy; however, these different tasks often require different isotopes. Imaging can be done with probes labeled with a positron ($\beta^+$) emitter (through PET) or a $\gamma$-emitter (through SPECT). Many promising therapeutic agents are $\beta^-$or $\alpha$-emitters that cannot be directly imaged with PET or SPECT. When developing drugs for targeted radioimmunotherapy it is beneficial to image biodistribution and uptake, but this currently requires modification of the drug for imaging.

Targeted $\alpha$-emitting isotopes have great therapeutic benefit due to the limited path length and high linear energy transfer of the $\alpha$-particle, as compared to electrons (Mulford *et al.*, 2005). Possible isotopes include $^{212}$Bi, $^{213}$Bi, $^{211}$At, $^{225}$Ac, and $^{230}$U (Holland *et al.*, 2010). Part of the appeal of $^{230}$U and $^{225}$Ac are the multiple $\alpha$-particles emitted from one initial decay (see the decay chains in figure 1). However, a limitation of alpha particle-based radiopharmaceuticals is that their emissions cannot be directly imaged using conventional nuclear medicine imaging methods.

Optical imaging has gained popularity in pre-clinical models due to the versatility of fluorescent and bio-luminescent probes. Optical imaging equipment is more widely available than nuclear imaging equipment but typically cannot image therapeutic agents without modifying the drug to have an imaging label. Optical methods typically have shorter

imaging times than nuclear imaging. However, the spatial resolution and fidelity of optical imaging is limited by the light scattering properties of tissue. In its simplest form, *in vivo* optical images are two-dimensional and have lower resolution than PET, but still produce useful quantitative information.

However, recently attention has been given to a mechanism by which radioactive decay can produce visible light suitable for optical imaging. Cerenkov radiation is a well-understood electromagnetic effect that occurs when a charged particle travels through a dielectric medium at a speed ($\upsilon$) greater than the speed at which light can travel in that medium ($c/n$), where $n$ is the index of refraction of the material. Many $\beta^+$and $\beta^-$emitters have been shown to produce Cerenkov light due to the emitted particles having an energy sufficient for $\upsilon > c/n$. This threshold is 263 keV for electrons and positrons in water. The intensity of Cerenkov radiation follows a $1/\lambda$ spectrum in the visible portion of the electromagnetic spectrum, which gives it a characteristic blueness. The spectral shape does not vary with any property of the decay or particle, rendering it not possible to distinguish between sources of Cerenkov light.

Cerenkov Luminescence Imaging (CLI) is an imaging modality that uses existing optical imaging systems, such as the IVIS (Caliper Biosciences, Alameda, CA), to image light produced by the energetic charged particles produced in many nuclear decays (Robertson *et al.*, 2009). Importantly, it has been shown that CLI provides quantitative data that correlates with PET (Ruggiero *et al.*, 2010) and SPECT (Hu *et al.*, 2010). While the measured optical data is two-dimensional, source depth can be inferred through spectral data (Spinelli *et al.*, 2010) and techniques have been developed to perform tomographic 3D reconstruction using homogeneous models (Li *et al.*, 2010) or heterogeneous models (Zhong *et al.*, 2011). The blue-dominated Cerenkov spectrum is subject to significant scattering in tissue, but it possible to use the Cerenkov light to excitep fluorophores, such as quantum dots, that subsequently give off light in wavelengths less subject to scattering (Liu *et al.*, 2010b). Recent work has shown that fluorophores can also be excitepd by Cerenkov light produced by external beam radiation (Axelsson *et al.*, 2011). While applications of CLI have not yet been fully explored, one of the clear applications is in pre-clinical imaging of isotopes that were previously not detectable by common imaging methods (Liu *et al.*, 2010a).

The only $\alpha$-emitting isotope known to the authors that has been imaged via CLI is $^{225}$Ac, which was shown to have significant light output that matched the expected Cerenkov spectrum (Ruggiero *et al.*, 2010). $^{225}$Ac has been shown to be effective at killing cancer cells (McDevitt *et al.*, 2001) and clinical trials are ongoing with targeted $^{225}$Ac agents (Rosenblat *et al.*, 2007). While $^{225}$Ac cannot be imaged via SPECT or PET, the daughters $^{221}$Fr and 213Bi have $\gamma$-ray lines at 218 keV and 440 keV (respectively). These lines allow for *ex vivo* $\gamma$-spectroscopy and SPECT imaging, although the $^{213}$Bi line is too energetic for some detectors (Woodward *et al.*, 2011). CLI could provide increased accessibility and decreased scan times for this isotope, as well as for other alpha-emitters for which imaging strategies have not yet been developed..

For an $\alpha$-particle to produce Cerenkov light it must have a kinetic energy far greater than typical decay energies due to its larger mass. This can be found from relativistic kinematics as shown in (1).

$$E_{\text{kin}}^{\min} = m_{\alpha}c^{2}\left(\frac{1}{\sqrt{1-\left(\frac{1}{n}\right)^{2}}}-1\right) \quad (1)$$

For water, with $n = 1.33$, the kinetic energy needed for an $\alpha$-particle to have a high enough velocity is 1926 MeV and for tissue with $n = 1.382$ it is 1673 MeV. The energy available in $\alpha$-decay is typically a few MeV, so $\alpha$-particles produced from decay will not directly produce Cerenkov light. How else could Cerenkov light be produced? The $\alpha$-particle ionizes electrons. However, the maximum energy of these electrons for elastic collisions with MeV-scale $\alpha$-particles is not near the Cerenkov threshold of 263 keV. Additionally, $\gamma$-rays can Compton scatter, producing free electrons. Many decays of these $\alpha$-emitting isotopes and their progeny produce $\gamma$-rays with many hundreds of keV of energy, so they are able to produce electrons above the Cerenkov threshold. This process produces only a small amount of Cerenkov light.

In this paper we demonstrate that the Cerenkov light detected from $^{225}$Ac is from daughter isotopes that decay through $\beta$-decay. We study the potential to image 4 other $\alpha$-emitting isotopes with CLI. Monte Carlo methods will be used to predict Cerenkov light production during the decay processes. This approach allows us to predict the temporal de-coupling between the decay of the initial isotope and the Cerenkov production. We conclude that 3 of the $\alpha$-emitting isotopes produce sufficient Cerenkov light to be imaged on time scales relevant to imaging studies.

## 2. Materials and Methods

### 2.1. Monte Carlo of Cerenkov Photon Yield

Cerenkov photon production was simulated using the Geant4 toolkit, version 4.09.03.p.02 (Agostinelli *et al.*, 2003). Geant4 is a C++ based Monte Carlo simulation toolkit that was developed for high energy physics but has recently been used in the medical community (Allison *et al.*, 2006). The toolkit offers great flexibility in geometry, data collection, and physics models. Generation of optical photons through the Cerenkov effect is a built in physics phenomenon, however, the user must define the optical properties of the materials used. The refractive index of water for the wavelengths 400 nm to 700 nm were taken from published tables (Hale and Querry, 1973).

Part of the advantage of Geant4 is the ability to choose physics models. The Penelope low energy electromagnetic models were used for Rayleigh scattering, photoelectric effect, Compton scattering, conversion, bremmstrahlung, and $e^{\pm}$-ionization. The Cerenkov production process was enabled for all charged particles. $\alpha$-particles also had elastic and inelastic hadronic processes enabled, multiple scattering via the hMultipleScattering process, and ionization through hLowEnergyIonisation. The default production cut for particles was

10 μm, with 10 nm for $\alpha$-particles and ions. For electrons this corresponds to a production threshold of about 14 keV in water, well below the Cerenkov threshold. Adequate modeling of the low energy electromagnetic processes is important because the rate of production of Cerenkov photons is tied to the energy of the particle along its entire path (Mitchell *et al.*, 2010). By using the low energy processes and a small step size the energy loss of the primary and secondary particles should be well modeled, including the point at which the energy is no longer above Cerenkov production.

Decays were generated at the center of a cube of water 5 cm on each side. For each isotope in the decay chain, 5 runs of 100,000 events were performed. In order to quantify the light production of only one decay stage, no subsequent radioactive decays were allowed for each event. Geant4 generated the decays based on branching fraction and energy information from the ENSDF database, including decays to excitepd levels and the de-excitation $\gamma$-rays produced. The Cerenkov photons from the primary decay products and secondary products (such as electrons from ionization and Compton interactions) were recorded. The mean and standard deviation of this set were then used in the decay Monte Carlo. Note that the standard deviations are larger than Poisson $(\sqrt{(N)})$ errors due to the random variations in decay mode, decay energy, and subsequent interactions.

### 2.2. Monte Carlo Decay Studies

Monte Carlo studies were developed in `C++` utilizing the `ROOT` toolkit, v 5.18/00b (Brun and Rademakers, 1997). Individual atoms were processed through the decay chain by randomly choosing a decay time according to the half-life of the element (Tuli, 1996). The chains used are shown in figure 1. If the isotope had two possible decays the path was randomly chosen according to the branching ratio. For every decay Cerenkov photons were generated. Using the mean and standard deviation from the Geant4 Monte Carlo simulation (as shown in figure 2) a Gaussian distribution was created representing the number of decays expected for $10^6$decays of that isotope. A number was randomly chosen from this distribution and divided by $10^6$to represent the number of photons for this given decay. There were two times recorded for these photons: the ‘global’ time from the start of the simulation and the time since the original isotope (ie, $^{225}$Ac) had decayed. The later will be referred to as the separation time. The Cerenkov production is normalized to the activity of the original isotope at the time, resulting in the units of Cerenkov photons per second per Becquerel. Because Becquerels are decays per second, this photon rate per decay rate is equivalent to photons per decay.

All reported rates are the production rate of Cerenkov photons between 400 nm and 700 nm. The surface radiance measured in an optical device will additionally depend on the geometry of the set up and the quantum efficiency of the camera. Such factors do not vary from one isotope to another. Hence, the ratio of Cerenkov photon production between two isotopes should be maintained when measuring surface radiance. $^{18}$F is used as a benchmark in this study since it is the most studied isotope with CLI.

# 3. Results

## 3.1. Photon Production of Individual Isotopes

Table 1 lists the mean and standard deviation of Cerenkov photons produced through 5 runs of 100,000 decays of the $\alpha$-emitting isotopes and their progeny. Each entry represents the Cerenkov light produced by that isotope alone without subsequent decays. The greatest number of Cerenkov photons are produced by high energy $\beta$-decay processes, with an average of over 30 Cerenkov photons produced per decay of $^{207}$Tl and $^{209}$Tl. Note that while $^{210}$Pb decays through $\beta^-$-emission, the maximum energy is far below the Cerenkov threshold. The isotopes that only decay through $\alpha$-emission show very low Cerenkov photon production. Querying the Geant4 data shows that this is due to nuclear de-excitation $\gamma$-rays Compton scattering and periodically producing electrons above the Cerenkov threshold. $^{211}$Po exhibits the highest Cerenkov photon count of the $\alpha$-emitting isotopes due to its 1% branching fraction to excitepd states of $^{207}$Pb which emit $\gamma$-rays with more than 500 keV of energy. The probability that these $\gamma$-rays will Compton scatter depends on the volume, that is, the greater the path the $\gamma$ travels in water, the higher the probability it will produce an electron.

While it is not a progeny of one of the $\alpha$-emitting isotopes under consideration, $^{18}$F was also simulated. The simulations resulted in 131,110.4 ± 676.5 Cerenkov photons per 100,000 decays. This is lower than some of the other $\beta$-emitting decays due to the low energy available in $^{18}$F decays, however, it is two orders of magnitude or more greater than the isotopes that only decay through $\alpha$-emission.

## 3.2. Decay Chain Photon Production

Figure 3 shows the number of Cerenkov photons per second emitted per Becquerel of parent isotope. The measurement was made during the first half of the $\alpha$-emitting isotopes' half-life, excluding any non-equilibrium time (discussed in section 3.3). Each isotope has been divided into the predominant sources of Cerenkov light. The contributions of some isotopes, such as $^{209}$Tl, is suppressed through the low branching fraction. Others, such as $^{207}$Bi, are limited by a long half-life. The rate of Cerenkov light production for both $^{230}$U and $^{211}$At is more 2 order of magnitude less than $^{18}$F.

## 3.3. Cerenkov Production Equilibrium

For Cerenkov Luminescence Imaging to be quantitatively useful for $\alpha$-emitters the measured light output must be proportional to the activity contained in a volume as it is for signals detected by PET and SPECT. Some of the decay chains exhibit a period of time where Cerenkov production increases before it remains proportional to the activity of the original isotope. Figure 4 shows this behaviour in the isotopes of interest. This time represents a 'global' time, the measurement beginning with a pure sample of the parent $\alpha$-emitter. For $^{225}$Ac there is a non-equilibrium period of about 10 hours, which is small compared to the half life of 10 days. $^{230}$U does not reach equilibrium within its half life of 20 days. $^{211}$At appears to be in equilibrium from the beginning, although it is populating the long-lived $^{207}$Bi state. Note that the spikes in photons are due to sporadic decays of $^{207}$Bi, which has a half life of 31.5 years. $^{213}$Bi has only a slight change in photon rate. For $^{212}$Bi the

production begins at about 25 photons/second/Bq and reaches equilibrium of 38 photons/second/Bq within 12 minutes.

### 3.4. Time Separation Between Initial Decay and Cerenkov Production

Because Cerenkov light is generated throughout the decay chain there can be a significant delay between the initial decay of the $\alpha$-emitting parent (such as $^{225}$Ac) and the measured light. Figure 5 shows the distribution for 4 of the considered isotopes. Note that this time is different from the previously measured time: a time of zero now corresponds to when a particular $\alpha$-emitting parent nucleus decayed. The isotopes either have a distribution dominated by prompt Cerenkov or an exponentially falling distribution. The mean time separation is small for the decay chains dominated by the prompt light: $^{213}$Bi is 17 seconds and $^{212}$Bi is 90 seconds. The other two isotopes have a high mean, with $^{230}$U at 40 minutes. Figure 6 shows the isotopic breakdown of two of the isotopes. $^{225}$Ac shows a small amount of prompt Cerenkov from the early $\alpha$-decays but is dominated by the $\beta$-decays occurring later in the chain. The mean of this distribution is 76.3 minutes and the peak occurs at 18 minutes. The equivalent distribution for $^{18}$F is a delta-function at t=0.

## 4. Discussion

This study demonstrates that Cerenkov luminescence imaging can be used to quantitatively image some $\alpha$-emitting isotopes as long as certain considerations are minded. $^{212}$Bi and $^{213}$Bi are considered $\alpha$-emitters for therapeutic applications but have a sizable branching fraction to $\beta^-$-decay, allowing them to be imaged via Cerenkov light. $^{230}$U and $^{211}$At have $\beta^\pm$-emitters in their decay chains, but the half-lives of these isotopes result in little Cerenkov light being produced on clinically relevant time scales. $^{225}$Ac can be imaged due to the $\beta^-$-emitters in its decay chain, but the interpretation the imaging data must take into account complicating time effects.

$^{212}$Bi and $^{213}$Bi are almost as simple to image with CLI as $^{18}$F. They are considered $\alpha$-emitters for therapeutic reasons but they are also $\beta^-$-emitters. These $\beta^-$-decays lead to direct and prompt production of Cerenkov light when the parent isotope decays. Both prompt decays are highly energetic, producing an order of magnitude more Cerenkov light than $^{18}$F does. However, both also have a production mechanism farther down the decay chain that leads to a period of non-equilibrium. For $^{213}$Bi this is the population of the $^{209}$Tl daughter that only causes a small change in the Cerenkov production. Because the half-life of $^{213}$Bi is only 46 minutes, the $^{209}$Pb ($t_{1/2}$=3.3 hours) never reaches equilibrium or contributes a significant amount of Cerenkov light while there is still a reasonable proportion of the parent isotope remaining. $^{212}$Bi has a larger contribution of Cerenkov light from its progeny, $^{208}$Tl. It takes only about 12 minutes for equilibrium to be reached, so selection of an appropriate imaging time is not difficult. Because the majority of the light is from the parental decay, the time separation is not a major concern. The average delay for $^{213}$Bi is about 17 seconds and for $^{212}$Bi it is 90 seconds.

This study indicates that $^{230}$U and $^{211}$At are unsuitable isotopes for CLI. The decay chains of both contain decays that would produce Cerenkov light, but they are blocked by half-lives of tens of years. Within the half-life of the parental isotope itself, Cerenkov light is produced

via Compton scattering of nuclear de-excitation $\gamma$-rays. This leads to very low levels of light (2 order of magnitude below $^{18}$F) and is dependent on the volume of tissue or water present. Additionally, the source of Cerenkov light will then be the position of the Compton scattering and not the site of the original decay. This interaction length is much longer than the mm scale path of a positron before annihilation, so this greatly reduces the resolution of CLI. In addition to the low level of light produced, $^{230}$U is a poor choice due to wide time separation between light and original decay (mean of 40 minutes) and not being in a state of equilibrium where Cerenkov light can be used to quantify the activity.

While the decay chain of $^{225}$Ac is more similar to $^{230}$U than either $^{212}$Bi or $^{213}$Bi, it it suitable for CLI as long as studies take into account the time effects present. The Cerenkov light is produced by progeny a few steps down in the decay chain, resulting in two effects. There is both a period where Cerenkov light production is not proportional to the quantity of activity present and there is a time delay between the decay of $^{225}$Ac and the observation of the subsequent Cerenkov light. The non-equilibrium period will not just be after production of the isotope, but will also occur after filtration stages in radio-chemistry. While the non-equilibrium effect could be observed by making measurements *in vitro*, the time separation cannot be easily measured since the Cerenkov spectrum does not depend on the energy of the initial particle, rendering it impossible to distinguish the Cerenkov photons coming from early in the decay chain from those produced at the end.

Both of these time effects must be taken into account when designing and analyzing CLI data *in vivo*. The greatest value of CLI is in reporting the location of a radiolabeled compound in a subject. Since the Cerenkov light is coming from daughter isotopes and not from the initial decay, CLI data will be reporting on the location of the daughter isotopes. This is not necessarily the location of the compound that had been labeled with the $\alpha$-emitter, which reduces the resolution already limited by optical scattering. Researchers must carefully consider the fate of the daughter isotopes through the entire chain to $^{209}$Bi. If the daughter isotopes remain in the same location (with respect to the spatial resolution of the study) as the radiolabeled compound this is less of a concern. A simple chelation of a targeting probe to $^{225}$Ac will result in the $^{221}$Fr daughter no longer being attached to the target of interest due to the high recoil energy of the $^{221}$Fr nucleus. This effect has already been explored with the intention of keeping the $\alpha$-emitting daughters at the target location through cellular internalization (McDevitt *et al.*, 2001), liposomal carriers(Sofou *et al.*, 2004), and nanoparticle delivery methods (Woodward *et al.*, 2011). If the $\beta$-emitting daughters are not conjugated to the target molecule after the initial $\alpha$-decay they may circulate freely before decaying and producing Cerenkov light. The amount of time this circulation would occur is described by the distribution in figure 5, resulting in an average circulation time of 76 minutes for $^{225}$Ac. Consequently, the Cerenkov light being imaged describes the bio-distribution of these secondary isotopes and provides little information on the effectiveness of the targeting mechanism. This will decrease the signal from the location of interest, increase the background, and potentially hide binding sites outside the location of interest. Sequestration of the daughters would eliminate this effect (and have other benefits (Miederer *et al.*, 2008)).

## Conclusion

Monte Carlo studies show that $^{212}$Bi and $^{213}$Bi can be directly imaged and quantified via CLI, while $^{225}$Ac can be imaged indirectly through its daughters. This has the potential to accelerate the screening of targeted $\alpha$-emitters in pre-clinical models, or to apply CLI clinically to monitor the distribution of radiopharmaceuticals. To our knowledge no *in vivo* Cerenkov imaging has been done of $\alpha$-emitting isotopes. We have shown that the results of these studies must be interpreted carefully due to time delays between the initial decay and the subsequent Cerenkov production.

## Acknowledgments

NLA is supported by the Weiland Family Fellowship administered through the Stanford Graduate Fellowships.

## References

Agostinelli S, Allison J, Amako K, Apostolakis J, Araujo H, Arce P, Asai M, Axen D, Banerjee S, Barrand G, et al. G4–a simulation toolkit. Nuclear Instruments and Methods in Physics Research Section A: Accelerators, Spectrometers, Detectors and Associated Equipment. 2003; 506:250–303.

Allison J, Amako K, Apostolakis J, Araujo H, Dubois P, Asai M, Barrand G, Capra R, Chauvie S, Chytracek R, et al. Geant4 developments and applications. Nuclear Science, IEEE Transactions on. 2006; 53:270–278.

Axelsson J, Davis SC, Gladstone DJ, Pogue BW. Cerenkov emission induced by external beam radiation stimulates molecular fluorescence. Medical Physics. 2011; 38:4127. [PubMed: 21859013]

Brun R, Rademakers F. ROOT: An object oriented data analysis framework. Nucl. Instrum. Meth. 1997; A389:81–86.

Hale GM, Querry MR, et al. Optical constants of water in the 200-nm to 200-um wavelength region. Appl. Opt. 1973; 12:555–563. [PubMed: 20125343]

Holland JP, Williamson MJ, Lewis JS. Unconventional nuclides for radiopharmaceuticals. Molecular Imaging. 2010; 9:1–20. [PubMed: 20128994]

Hu Z, Liang J, Yang W, Fan W, Li C, Ma X, Chen X, Ma X, Li X, Qu X, et al. Experimental cerenkov luminescence tomography of the mouse model with SPECT imaging validation. Optics Express. 2010; 18:24441–24450. [PubMed: 21164791]

Li C, Mitchell GS, Cherry SR. Cerenkov luminescence tomography for small-animal imaging. Optics Letters. 2010; 35:1109–1111. [PubMed: 20364233]

Liu H, Ren G, Miao Z, Zhang X, Tang X, Han P, Gambhir SS, Cheng Z. Molecular optical imaging with radioactive probes. PLoS ONE. 2010a; 5:e9470. [PubMed: 20208993]

Liu H, Zhang X, Xing B, Han P, Gambhir SS, Cheng Z. Radiation-Luminescence-Excited quantum dots for in vivo multiplexed optical imaging. Small. 2010b; 6:1087–1091. [PubMed: 20473988]

McDevitt MR, Ma D, Lai LT, Simon J, Borchardt P, Frank RK, Wu K, Pellegrini V, Curcio MJ, Miederer M, et al. Tumor therapy with targeted atomic nanogenerators. Science. 2001; 294:1537–1540. [PubMed: 11711678]

Miederer M, Scheinberg DA, McDevitt MR. Realizing the potential of the actinium-225 radionuclide generator in targeted alpha particle therapy applications. Advanced Drug Delivery Reviews. 2008; 60:1371–1382. [PubMed: 18514364]

Mitchell GS, Gill RK, Cherry SR. Comments on 'cerenkov radiation allows in vivo optical imaging of positron emitting radiotracers'. Physics in Medicine and Biology. 2010; 55:L43. [PubMed: 20736495]

Mulford DA, Scheinberg DA, Jurcic JG. The promise of targeted alpha-Particle therapy. J Nucl Med. 2005; 46:199S–204. [PubMed: 15653670]

Robertson R, Germanos MS, Li C, Mitchell GS, Cherry SR, Silva MD. Optical imaging of cerenkov light generation from positron-emitting radiotracers. Physics in Medicine and Biology. 2009; 54:N355–365. [PubMed: 19636082]

Rosenblat TL, McDevitt MR, Pandit-Taskar N, Carrasquillo JA, Chanel S, Frattini MG, Larson SM, Scheinberg DA, Jurcic JG. Phase i trial of the targeted alpha-particle nano-generator actinium-225 (225ac)-hum195 (anti-cd33) in acute myeloid leukemia (aml). ASH Annual Meeting Abstracts. 2007; 110:910.

Ruggiero A, Holland JP, Lewis JS, Grimm J. Cerenkov luminescence imaging of medical isotopes. Journal of Nuclear Medicine: Official Publication, Society of Nuclear Medicine. 2010; 51:1123–1130.

Sofou S, Thomas JL, yin Lin H, McDevitt MR, Scheinberg DA, Sgouros G. Engineered liposomes for potential alpha-particle therapy of metastatic cancer. Journal of Nuclear Medicine: Official Publication, Society of Nuclear Medicine. 2004; 45:253–260.

Spinelli AE, D'Ambrosio D, Calderan L, Marengo M, Sbarbati A, Boschi F. Cerenkov radiation allows in vivo optical imaging of positron emitting radiotracers. Physics in Medicine and Biology. 2010; 55:483–495. [PubMed: 20023328]

Tuli JK. Evaluated nuclear structure data file. Nuclear Instruments and Methods in Physics Research Section A: Accelerators, Spectrometers, Detectors and Associated Equipment. 1996; 369:506–510.

Woodward J, Kennel SJ, Stuckey A, Osborne D, Wall J, Rondinone AJ, Standaert RF, Mirzadeh S. LaPO(4) nanoparticles doped with actinium-225 that partially sequester daughter radionuclides. Bioconjugate Chemistry. 2011

Zhong J, Qin C, Yang X, Zhu S, Zhang X, Tian J. Cerenkov luminescence tomography for in vivo radiopharmaceutical imaging. International Journal of Biomedical Imaging. 2011; 2011:1–6.

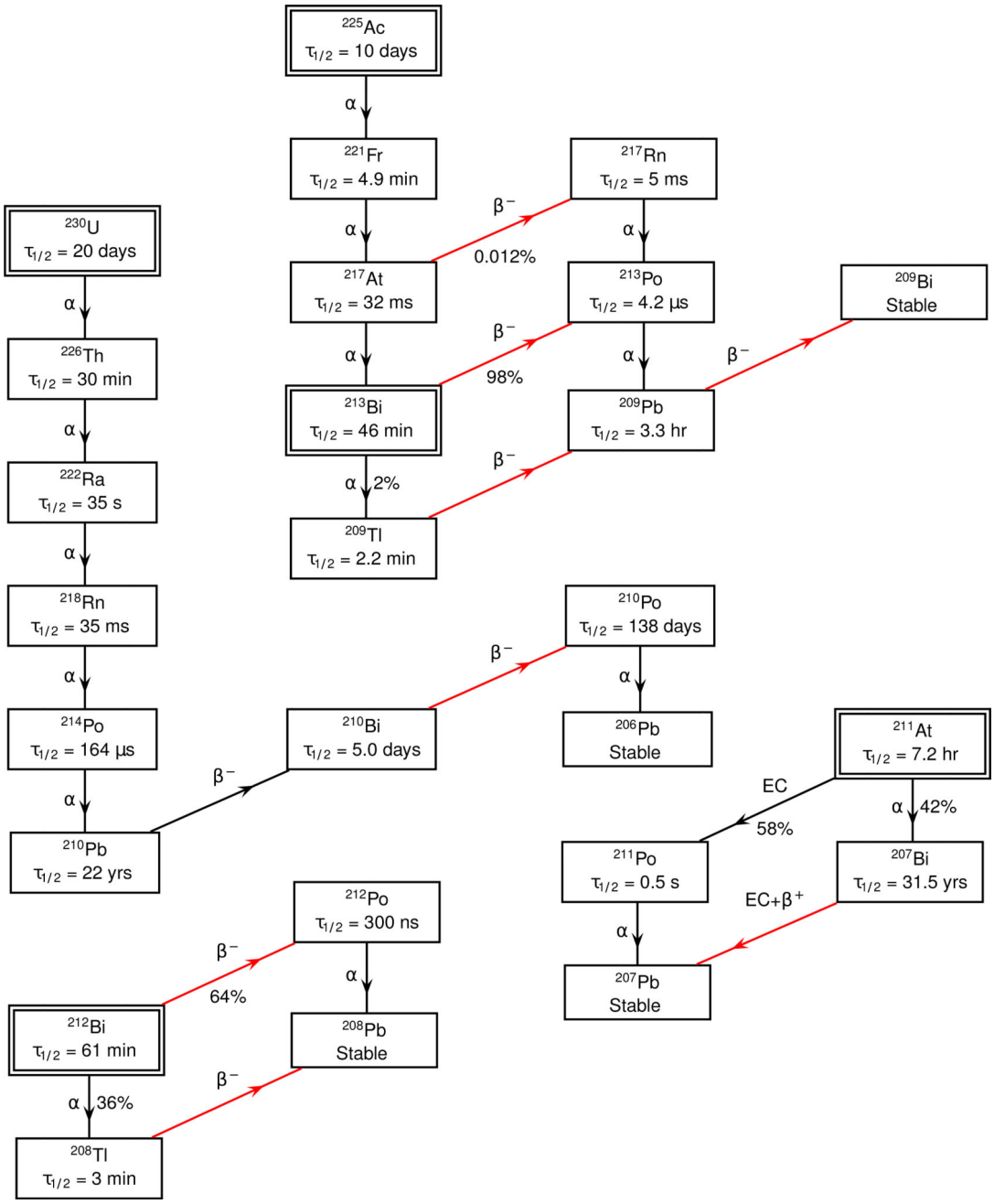


**Figure 1.**

Decay chains of considered isotopes. Double boxed isotopes are the starting points. Red lines indicate pathways that directly produce Cerenkov light.

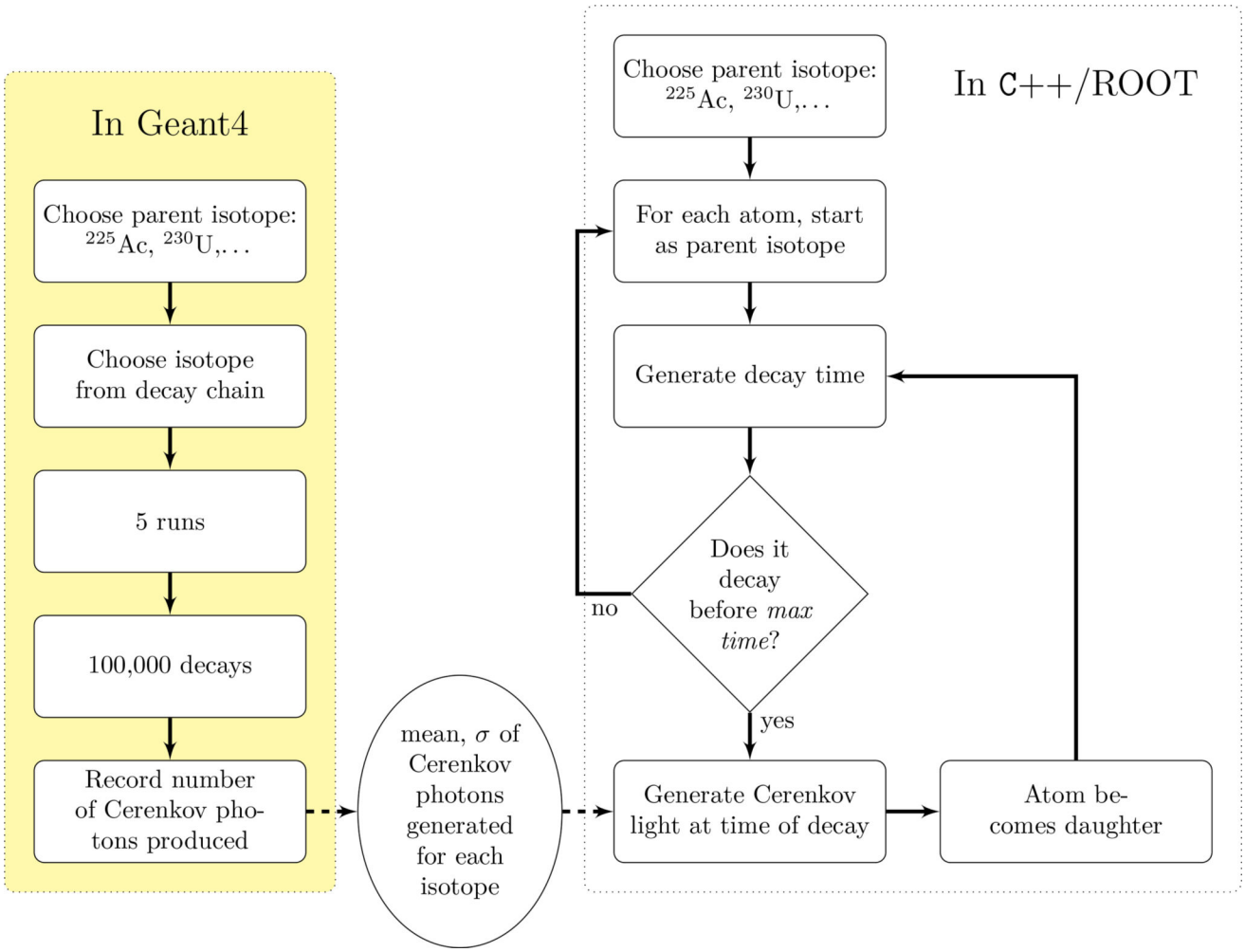


**Figure 2.**

The Monte Carlo simulation had two stages. We used Geant4 to establish the Cerenkov photon production for each isotope. Then we generated the time dependence of the Cerenkov production for the entire decay chain, using the information from the first step.

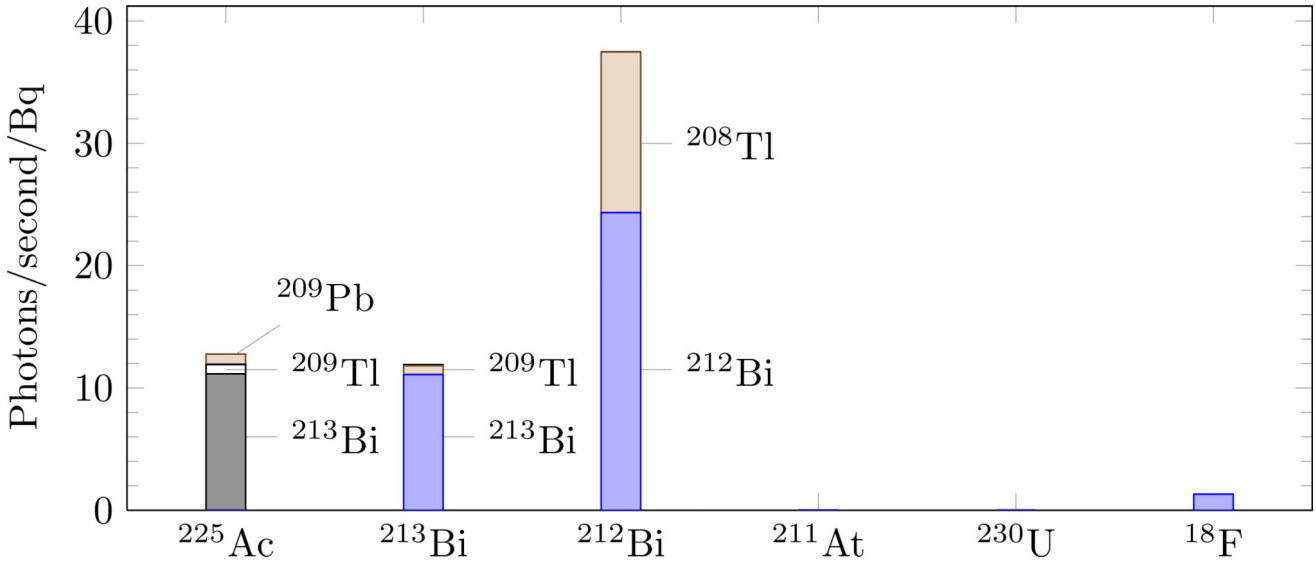


**Figure 3.**

Average Cerenkov production for the six isotopes as predicted by Monte Carlo. Dominant sources of Cerenkov photons are annotated. Cerenkov production by $^{211}$At and $^{230}$U are 2 orders of magnitude less than $^{18}$F.

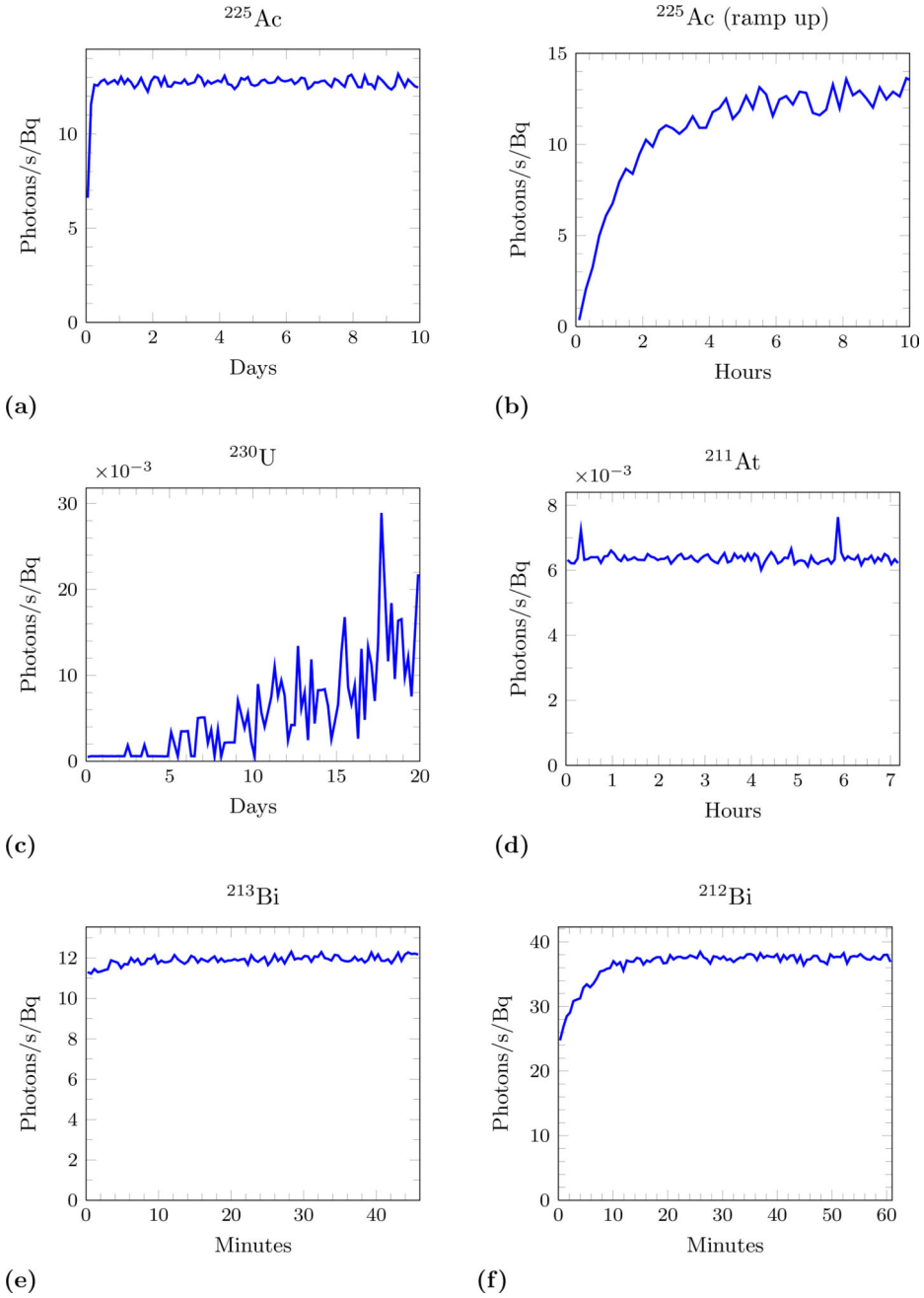


**Figure 4.**

Cerenkov photon production rate (normalized to activity) as a function of time from a pure sample. (a) and (b) shows two different time periods for $^{225}$Ac. Note the x-axis varies in scale to account for the different half-lives of the isotopes and that the y-axis of (c) and (d) has a factor of $10^{-3}$.

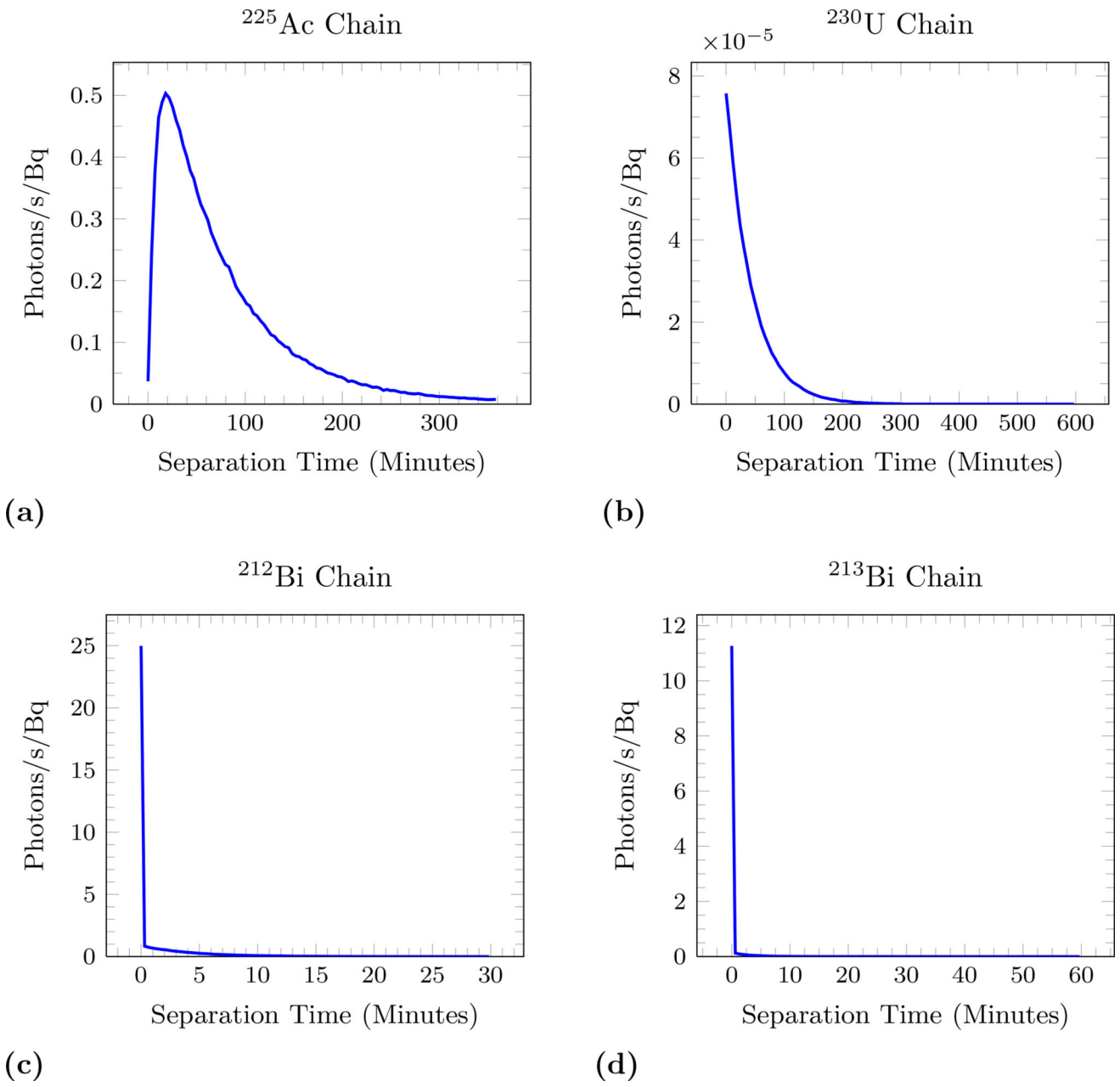


**Figure 5.**

Separation time for the 4 isotopes that do not only produce prompt light. Separation time represents the time between the initial decay of the parent $\alpha$-emitter and the subsequent production of Cerenkov light. Note that the y-axis of (b) has a factor of $10^{-5}$.

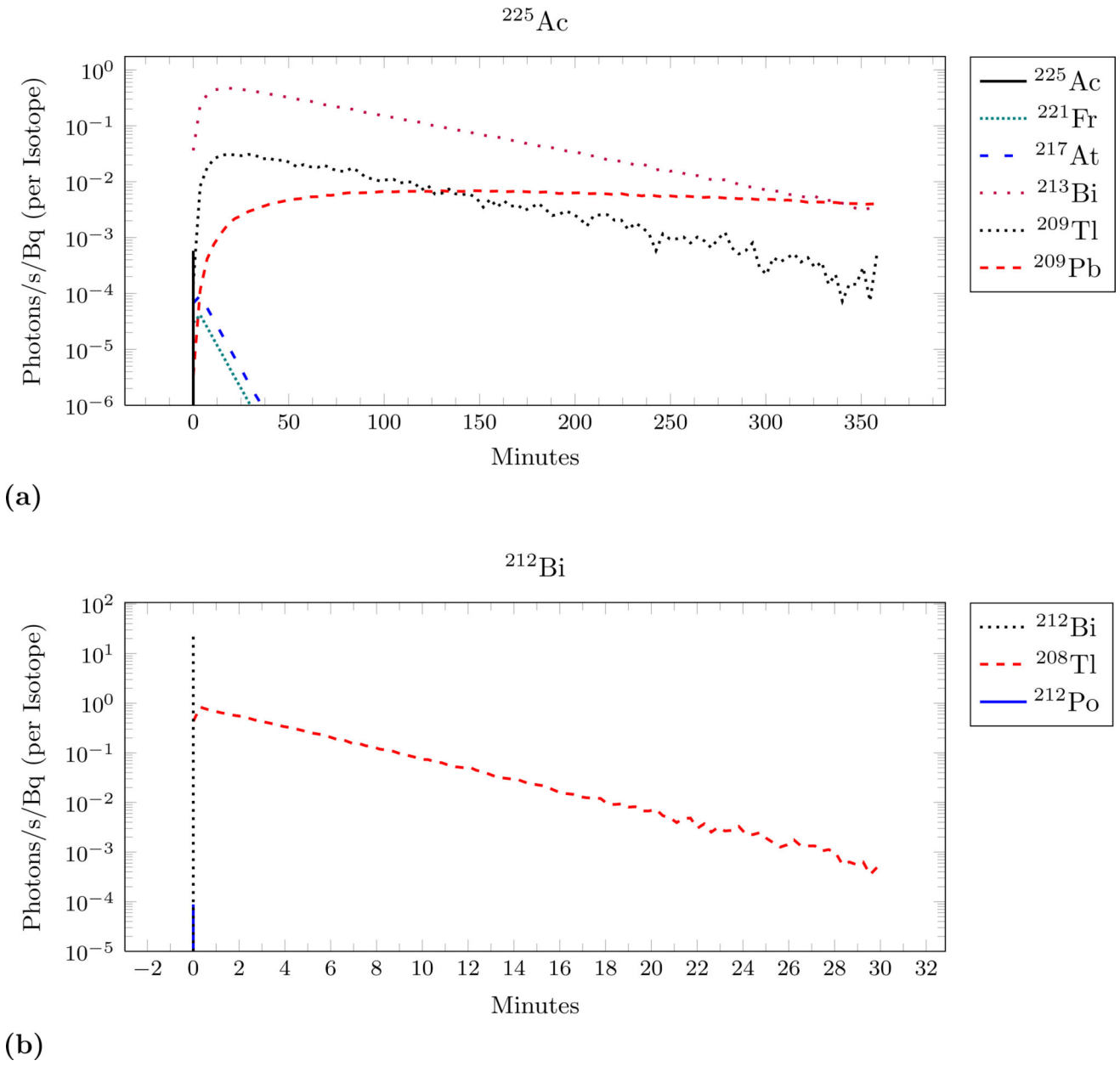


**Figure 6.**

The different isotopes in the decay chain are responsible for different portions of the time separation. This shows the sources of the distributions from figure 5 parts (a) and (c) on logarithmic y-axis. Vertical lines represent the delta-functions of prompt light occuring at t=0.

**Table 1**

Number of Cerenkov Photons generated for 100,000 decays of the given isotope. Displayed values are mean and standard deviation taken from 5 simulations of 100,000 events.

| $^{225}$Ac Decay Chain | | $^{230}$U Decay Chain | | $^{211}$At Decay Chain | |
|---|---|---|---|---|---|
| $^{225}$Ac | 57.4±20.6 | $^{230}$U | 3.2±7.2 | $^{211}$At | 125.8±19.3 |
| $^{221}$Fr | 13.2±5.6 | $^{226}$Th | 2.8±4.1 | $^{211}$Po | 870.2±85.5 |
| $^{217}$At | 28.0±23.5 | $^{222}$Ra | 17.6±19.9 | $^{207}$Bi | 583,482.0±6902.1 |
| $^{217}$Rn | 0±0 | $^{218}$Rn | 24.8±8.2 | $^{212}$Bi Decay Chain | |
| $^{213}$Bi* | 1,107,725.8±1889.3 | $^{214}$Po | 5.0±7.1 | | |
| $^{209}$Tl | 3,616,482.4±7763.8 | $^{210}$Pb | 0±0 | $^{212}$Bi | 2,430,437.2±7403.2 |
| $^{213}$Po | 0±0 | $^{210}$Bi | 816,719.4±6327.1 | $^{208}$Tl | 3,475,761.0±11,864.1 |
| $^{209}$Pb | 83,270.4±529.6 | $^{210}$Po | 0±0 | $^{212}$Po | 9.6±19.9 |

*$^{213}$Bi and below are also the $^{213}$Bi decay chain.